Modeling of the Test Fixtures to Improve the HBC Channel Interpretation

M. D. Pereira, G.A. Alvarez, F. R. de Sousa
Radio Frequency Research Group
Federal University of Santa Catarina - UFSC
Florianópolis-SC, Brazil
{maicondeivid, g.a.alvarez, rangel}@ieee.org

***Abstract* —The Human Body Communication (HBC) presents security, power and interference advantages over common RF methods, which makes it an interesting alternative to implement body area networks. This paper presents a modeling attempt that takes into account the fixture influences present on the HBC channel characterization. An extended model, that includes the traditional primary channel model clearly identified, and the model of measurement accessories is proposed to better explain the measured channel responses. The model was tested against channel measurement and good results were obtained for frequencies below 70 MHz.**

Keywords — wireless body area networks, human body communication; HBC; capacitive coupling; test fixtures.

I. INTRODUCTION

The Human Body Communication (HBC) technology was firstly proposed by Zimmerman in 1995 [1], and has recently emerged as an alternative that could overcome most of the WBAN (Wireless Body Area Networks) challenges related to low power, high data rates and high security devices [2]. In HBC the information signal is coupled to the body through an electrostatic field via electrodes and is captured in another part of the body using similar electrodes. The HBC operating frequency is usually between 0.1 MHz and 100 MHz, to avoid electromagnetic interference and minimize the radiation of the signal out of the body, respectively. These characteristics make HBC less sensitive to electromagnetic interference, provides higher data communication security, presents higher spectral efficiency and potential of eliminating power-hungry RF front-end circuits [1], [3].

Regarding the HBC coupling method, there are two options: the capacitive coupling and the galvanic coupling. In the galvanic coupling [4], a pair of electrodes is in contact with the skin at the transmitter (TX) and couples a differential signal that induces galvanic currents. The signals are captured by another pair of electrodes in contact with the skin at the receiver (RX), as shown in Fig. 1 (a). In the capacitive coupling one of the transmitter electrodes is attached to the skin, and the other is kept floating. In this way, the transmitter generates an electric potential, inducing an electric field in the body that is sensed by the receiver electrodes arranged in the same way. The floating electrodes are coupled to ground through the air, creating a return path, while the signal electrodes in contact with the skin create the signal forward path [5], as shown in Fig. 1 (b). This article focuses on the capacitive coupling method.

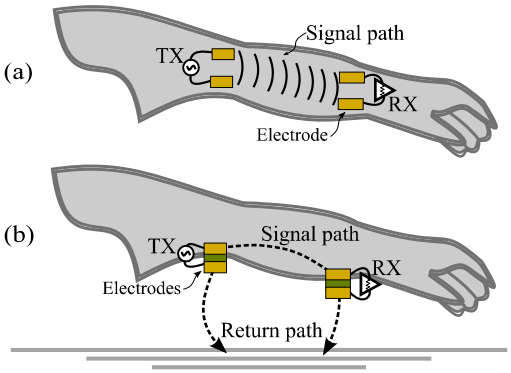

Fig. 1. HBC coupling methods: (a) galvanic and (b) capacitive.

The correct channel modeling is essential to help the design of transceivers that meet the requirements of WBANs. However, since the proposal of HBC, they still are a subject of discussion. Among recent attempts that simultaneously address characterization and modeling for the capacitive HBC are the works of Callejón *et al.* [4], Xu *et al.*[6] and Bae *et al.* [7]. Callejón *et al.* proposed a body channel transmission model based on skin impedance and admittance derived from skin cell dimensions and electrical characteristics. Bae *et al.* presented a channel model based on the theoretical solution of the electrical field from an infinitesimal dipole on the surface of the body, describing the path loss according to distance and frequency. Xu *et al.* extracted a distributed-network circuit model from 3D electromagnetic (EM) simulation results performed on different body members. Overall, these references either lack an explicit model of all the channel parts, or do not make a substantial assessment of the test fixture influences on the measurements results used to validate the proposed models, leading to different modeling results. To clarify these issues, this paper proposes the division of the primary HBC channel in an intrinsic and an extrinsic part to facilitate its modeling, and improves the models available in the literature by suggesting the addition of the measurement setup influences to an HBC extended model.

The paper is organized as follows, Section II reviews the primary channel, separating it in its static and dynamic parts, Section III models the channel measurement setup and Section IV compares measurements to the proposed extended model.

II. Primary Channel Modeling

Perhaps the most crucial aspect during channel characterization and modeling in HBC is to identify the correct primary channel. The primary capacitive HBC channel can be divided in an intrinsic and an extrinsic part. The intrinsic part is the direct path through the body between the signal electrodes, as show in Fig. 2, that should be modeled basically by the tissues electrical properties, and is represented by C_{body} and R_{body}. This intrinsic section can be considered independent of the external conditions, being only dependent on distance of propagation over the body and the tissues properties.

In [6], the intrinsic part of the channel is modeled by the cascading of unit length RC circuit blocks for arms and torso, as shown in Fig. 3, estimated from 3D EM simulations. The components $C_{(arm,\ chest,\ torso)}$ and $R_{(arm,\ chest,\ torso)}$ represent the composite effect of the body tissues in each segment. Each unit block also includes C_{leak}, takes into account the coupling that appears from the body segments to the ground. This model is valid to represent generic body path measurements, since there is no need to do changes to the tissues parameters to account for different subjects, as this usually has a negligible effect on the channel response [5], [8]. It will be adopted as the reference for the intrinsic part of the primary channel model presented in this article, substituting R_{body} and C_{body} in Fig. 2.

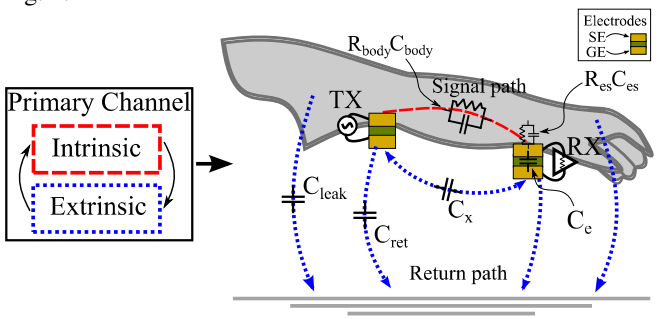

Fig. 2. Capacitive coupling HBC primary channel with its intrinsic and extrinsic parts (GE = Ground Electrode, SE = Signal Electrode).

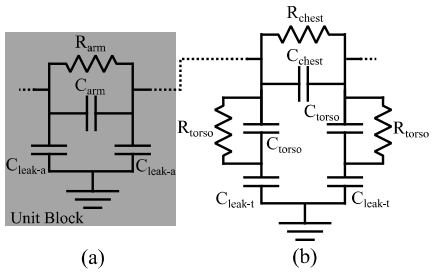

Component values

R_{arm}	65 Ω	R_{chest}	500 Ω
C_{arm}	25 pF	C_{chest}	3.5 pF
$C_{leak\text{-}a}$	0.7 pF	R_{torso}	600 Ω
$C_{leak\text{-}t}$	15 pF	C_{torso}	4 pF

Fig. 3. Distributed-network circuit model representing a (a) 10 cm unit block for the arm and (b) 40 cm unit block for the torso [6].

The extrinsic part of the channel is the return path through the air between the external ground plane and the ground electrodes, modeled by C_{ret} and C_x, and the signal leakage directly from the body to the electrodes or the ground plane, modeled by C_{leak}, as show in Fig. 2. The interfaces between transceivers and the body, *i.e.,* the electrodes pairs are also parts of the extrinsic channel, and are represented by C_e, C_{es} and R_{es}, the inter-electrode capacitance and the parallel RC electrode-skin contact model, respectively. The extrinsic portion of the channel is dependent on the environment, the distance from the ground, the electrodes and its contact with the skin. These parts must be modeled considering the conditions of tests performed on the primary channel, unlike the intrinsic part, as stated before.

The ground coupling capacitance, C_{ret}, was calculated using an empirical approximation for plates separated by large distances following the method presented in [9], and compared with C_{ret} extracted through 1-port 3D EM finite element method (FEM) simulation of copper square electrodes with side length L = 2 cm and of a variable distance h from the ground. The results appear in Fig. 4, and show that the largest discrepancy is of 15.5 % for the estimated capacitance, with the C_{ret} value decreasing for large distances from ground, and asymptotically converging to a minimum limit value around C_{ret} = 870 fF, for h > 50 cm.

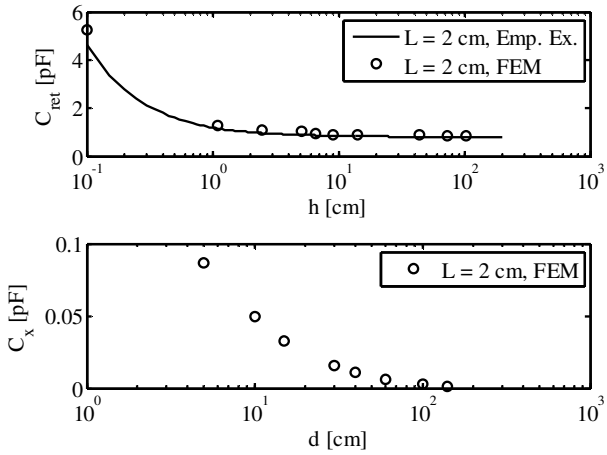

Fig. 4. Ground coupling capacitance, C_{ret}, according to distance h from ground plane for empirical expression (Emp. Ex.) and 3D EM simulation (FEM). Cross electrode capacitance, C_x, according to separation d between ground electrodes.

The cross capacitance C_x, was extracted from 2-port 3D EM simulations of the electrodes with length L = 2cm, horizontal distance between plates of 150 cm > d > 5 cm and height from ground plane of h = 75 cm. The obtained value for C_x is presented in Fig. 4. Despite being much lower than C_{ret}, it still has a non-negligible effect on the channel response as will be shown ahead.

The leakage capacitances C_{leak} were extracted through 3D EM simulations for arms and torso segments in [6] for each unit block. The simulation conditions were similar to the measurement circumstances of this work, thus, the values for the leakage capacitances were adopted in the model presented in this article. The coupling from the body parts to the ground electrodes influence can be neglected in the presented model [10].

The inter-electrode impedance is calculated noticing that the electrode pair in this work has a vertical structure, as show in Fig. 2, creating a capacitance between ground (GE) and signal (SE) electrodes that can be calculated by $C_e = \varepsilon L^2/d$. Where, ε is the permittivity of the material between the electrodes, L is the length of the electrodes and d is the separation between them. For a 4 cm^2 copper electrodes, with a 0.15 cm thick FR4 dielectric, the capacitance is C_e = 11.3 pF.

The electrode-skin impedance effect is accounted for within intrinsic path model structure in [6], adopted in the paper, by means of modified unit blocks for the region were the signal is injected into the skin. The modified unit length block is equal to the arm block presented in Fig. 3(a), only substituting C_{arm} and R_{arm} by $C_{injection}$ = 5.5 pF and $R_{injection}$ = 250 Ω.

With all the parameters of Fig. 2 defined, a 2-port S-parameters simulation of the primary channel model was performed for different separations between Rx and Tx electrodes, and with a total body length of 70 cm for each arm and 40 cm for the torso. The results are presented in Fig. 5 and show a channel response with a high-pass profile due to the return path capacitive behavior. In low frequency there is a small gain difference between the distances of propagation over the body, but as the frequency increases the gain has a higher dependence on distance. This is the channel response to be the expected if the test fixtures are neglected. However, as will be seem in the next section, the model has to include the test fixture to represent channel measurement results on conventional laboratory equipment.

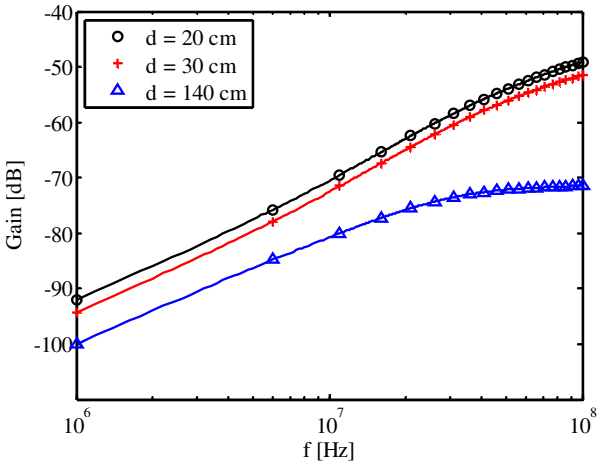

Fig. 5. Primary channel model gain simulation for three propagation distances over the body: d = 20 cm, 30 cm and 140 cm .

III. Test Fixture Model

Modeling simplifications or limitations could be one of the causes for some models inability to reproduce measurement results. However, the divergences could also be related to the omission of fixtures influences. For the models of [6] and [10], the circuit simulation results were compared to measurements taken from setups that did not address the issue of grounded equipment at the receiver. The models of [4] and [7] were tested against measurements on setups were the fixture non-idealities were not fully considered, this could be essential to explain the measured results.

In this work, the test setup includes a two-port Rohde & Schwarz ZVB Vector Network Analyzer (300 KHz - 8 GHz), with FTB-1-6- Mini-circuits baluns used to decouple the HBC ground from the VNA ports ground. In this configuration, potential source of influences, are the transitions between cables and electrodes, and the balun transformers itself.

The transition of the coaxial cable to electrodes is similar to the coaxial-to-PCB transitions and its basic model, presented in Fig. 6 (a), has an L_tC_t circuit, where L_t was approximated by the inductance of a wire with 1 cm length and 0.1 cm diameter, and the capacitance C_t was neglected given its low value, in the order of fF, much lower than the baluns output capacitances.

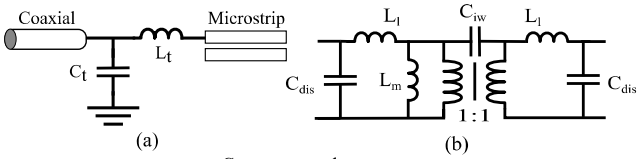

Component values

C_{iw}	27.2 pF	L_l	420 nH	L_t	6 nH
C_{dis}	12.3 pF	L_m	200 uH	C_t	-

Fig. 6. Models for (a) coaxial to microstrip transition and (b) balun transformer.

The balun is model is shown in Fig. 6(b) [11] with its components value, extracted experimentally [12]. The inductance L_l is estimated with an impedance measurement on the primary, while the secondary is shorted. An open circuit impedance measurement provides L_m. This measurement was also used to obtain the value for C_{dis}, since in high frequency the open impedance resonates and becomes capacitive. The capacitance C_{iw} is extracted by measuring the impedance between the primary and the secondary when both are shorted. The measurements were made using an Agilent 4294A LCR meter with the Fixture 16047E properly calibrated.

IV. Extended Channel Model

The extended channel model combines the primary channel and test fixture models presented in the previous sections, as shown in Fig. 7. The channel response over frequency for the extended model, the primary channel alone and channel measurements appears in Fig. 8 for the propagation distance of 30 cm, with the transmitter electrodes placed on the wrist and the receiver electrodes placed 30 cm away on the same arm. Additional channel measurement results can be found in [8].

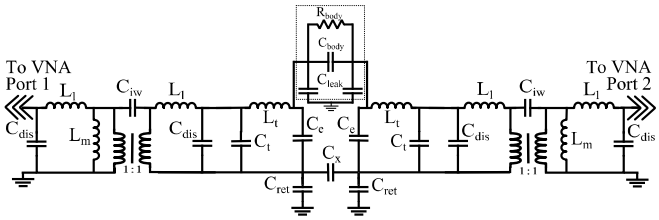

Fig. 7. Extended HBC channel model: primary channel and fixtures model.

Notice that the difference in gain between measurement results and the extended model is always lower than 5.5 dB for frequencies up to 70 MHz. This divergence could be due to the correct C_{iw}, that effectively boosts the signal gain [13], being slightly lower than its measured value. Also, there is the assumption of fixed values for the components that actually present some dependence on frequency over the range investigated. Above 70 MHz, the model and measurements divergence possibly arises from some non-modeled resonance or discontinuity [6]. However, the results present a good agreement and show that adding the fixture model it is possible to explain the measurement results with conventional equipment and accessories, indicating the strong influence of the measurement setup on the primary channel correct response, that should be almost 50 dB lower and present a high-pass profile, as shown by the primary channel model.

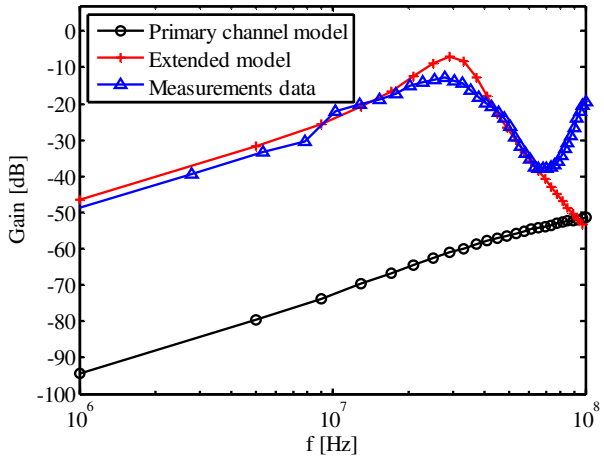

Fig. 8. Measurement and models simulation results for a channel propagation distance of 30 cm.

V. CONCLUSION

This work approached the channel modeling problem by suggesting that the issues found in the models available in the literature are not strictly connected to the primary channel model itself, but to the omission of the influences of test fixture on the channel measurement. Initially, it was proposed the division of the primary HBC channel in two parts: intrinsic and extrinsic. This helped to identify and represent the basic primary channel and proceed to the test fixture modeling and grouping of these models to form an extended model. Despite being simple, the models adopted were based on the physical explanation of the components and phenomena present in the setup and primary channel and gave a useful view of the channel expected behavior. The model verification showed that the test fixture indeed boosts the primary channel gain and changes the channel frequency profile, making difficulty for the available models, that did not include fixture, to reproduce measurement results. The presented model helps to properly describe the behavior of the channel measurements, being useful to understand some of the physical mechanisms in the channel response.

ACKNOWLEDGMENT

The authors would like to thank to Kaléo Turnes Silvestri for the assistance on channel measurements and CNPq Brazil for the financial support.

REFERENCES

[1] Zimmerman, T. G., “Personal Area Networks: Near-field intra-body communication,” M.S. Thesis, MIT Media Laboratory, Cambridge, MA, Sept. 1995.

[2] Hanson, M.A; Powell, H.C.; Barth, AT.; Ringgenberg, K.; Calhoun, B.H.; Aylor, J.H.; Lach, J., "Body Area Sensor Networks: Challenges and Opportunities," Computer , vol.42, no.1, pp.58,65, Jan. 2009.

[3] S.-H. Pun; Y.-M. Gao; P.U. Mak; M.-I Vai; M. Du, "Quasi-Static Modeling of Human Limb for Intra-Body Communications With Experiments," Information Technology in Biomedicine, IEEE Transactions on, Nov. 2011.

[4] Amparo Callejon, M.; Naranjo-Hernandez, D.; Reina-Tosina, J.; Roa, L.M., "Distributed Circuit Modeling of Galvanic and Capacitive Coupling for Intrabody Communication," Biomedical Engineering, IEEE Transactions on, Nov. 2012.

[5] Lucev, Z.; Krois, I; Cifrek, M., "A Capacitive Intrabody Communication Channel from 100 kHz to 100 MHz," Instrumentation and Measurement, IEEE Transactions on , vol.61, no.12, pp.3280,3289, Dec. 2012.

[6] R. Xu; H. Zhu; J. Yuan, "Electric-Field Intrabody Communication Channel Modeling With Finite-Element Method," Biomedical Engineering, IEEE Transactions on, March 2011.

[7] J. Bae; H. Cho; K. Song; H. Lee; H.-J. Yoo, "The Signal Transmission Mechanism on the Surface of Human Body for Body Channel Communication," Microwave Theory and Techniques, IEEE Transactions on, March 2012.

[8] Pereira, M.D.; Silvestri, K.T.; de Sousa, F.R., "Measurement results and analysis on a HBC channel," Medical Measurements and Applications (MeMeA), 2014 IEEE International Symposium on, vol., no., pp.1,6, 11-12 June 2014.

[9] Ruoyu Xu; Wai Chiu Ng; Hongjie Zhu; Hengying Shan; Jie Yuan, "Equation Environment Coupling and Interference on the Electric-Field Intrabody Communication Channel," Biomedical Engineering, IEEE Transactions on , vol.59, no.7, pp.2051,2059, July 2012.

[10] N. Cho; Yoo, J.; S.-J. Song; J. Lee; S. Jeon; H.-J. Yoo, "The Human Body Characteristics as a Signal Transmission Medium for Intrabody Communication," Microwave Theory and Techniques, IEEE Transactions on, May 2007.

[11] Colonel Wm. T. McLyman, "Transformer And Inductor Design Handbook", Third Edition, Revised and Expanded, Kg Magnetics, Inc. Idyllwild, California, U.S.A, 2004.

[12] Agilent Techonologies, "Impedance Measurement Handbook: A Guide to Measurement Technology and Techniques", December 2003.

[13] Sakai, J.; Lin-Sheng Wu; Hu-Cheng Sun; Yong-Xin Guo, "Balun's effect on the measurement of transmission characteristics for intrabody communication channel," Microwave Workshop Series on RF and Wireless Technologies for Biomedical and Healthcare Applications (IMWS-BIO), 2013 IEEE MTT-S International , vol., no., pp.1,3, 9-11 Dec. 2013.